Light Metals 2012 *Edited by: Carlos E. Suarez*
TMS (The Minerals, Metals & Materials Society), 2012

EXPERIMENTAL AND THEORETICAL STUDY ON THE FLUIDIZATION OF ALUMINA FLUORIDE USED IN THE ALUMINUM SMELTER PROCESSES

Paulo Douglas S. de Vasconcelos[1], André L. Amarante Mesquita[2]
[1]Albras - Alumínio Brasileiro S/A, Barcarena-PA, Brazil
[2]Federal University of Pará, Belém-PA, Brazil.

Keywords: Fluidized bed, Minimum fluidization velocity, Permeameter, Maximum pressure drop

Abstract

Fluidization is an engineering unit operation that occurs when a fluid (liquid or gas) ascends through a bed of particles, and these particles get a velocity of minimum fluidization V_{mf} enough to stay in suspension, but without carrying them in the ascending flow. As from this moment the powder behaves as liquid at boiling point, hence the term "fluidization". This operation is widely used in the aluminum smelter processes, for gas dry scrubbing (mass transfer) and in a modern plant for continuous alumina pot feeding (particles' momentum transfer). The understanding of the alumina fluoride rheology is of vital importance in the design of fluidized beds for gas treatment and fluidized pipelines for pot feeding.
This paper shows the results of the experimental and theoretical values of the minimum and full fluidization velocities for the alumina fluoride used to project the state of the art round non-metallic air-fluidized conveyor of multiples outlets.

Introduction

Gas-solid flow occurs in many industrial operations. The majority of chemical engineering units operations, such as drying, separation, adsorption, pneumatic conveying, fluidization and filtration involve gas-solid flow.
Poor powder handling in an industrial process operation may result in a bad performance, leading to errors in the mass balance, erosion caused by particles impacts in the pipelines, attrition and elutriation of fines overloading the bag houses. Lack of a good gas-solid flow rate measurement can cause economic and environmental problem due to airborne particles.
This paper focuses on the applications of powder technology related to the aluminum smelters processes such as dry scrubbing of gases and pot feeding to produce primary aluminum.
To optimize the residence time in the gas-adsorption process and minimize the energy consumption in the pot feeding, the precise determinations of the minimum and full fluidization velocities as well as the aerated and non-aerated angle of repose of the alumina should be mandatory.

Fundamentals of powder fluidization

In the powder processes discussed above, it is important to know the hydrodynamic behavior of the particles in fluidized beds. It is known that the fluidization behavior of a gas-solid bed depends on the particle diameter and density. Geldart (1973) classified powders into four types: C, A, B and D, based on their fluidization behavior. Geldart's diagram is illustrated in figure 1.
The fluidized bed regime map is illustrated in figure 2.

Group C particles have small diameters and are very difficulty to fluidize. Channeling the bed of particles becoming difficult to determine the minimum fluidization velocity – ultrafine alumina $d_p < 20\mu m$. Group A particles are aeratable and readily fluidize – fine alumina $d_p \sim 40.5\mu m$. Group B alumina forms a bubble bed after the fixed bed with increasing gas velocity - $d_p > 70\mu m$. Group D particles are relatively large bean-shape particles - $d_p \sim 1000\mu m$. This bed of particles is spoutable, re-circulating the particles in the fluidized bed.

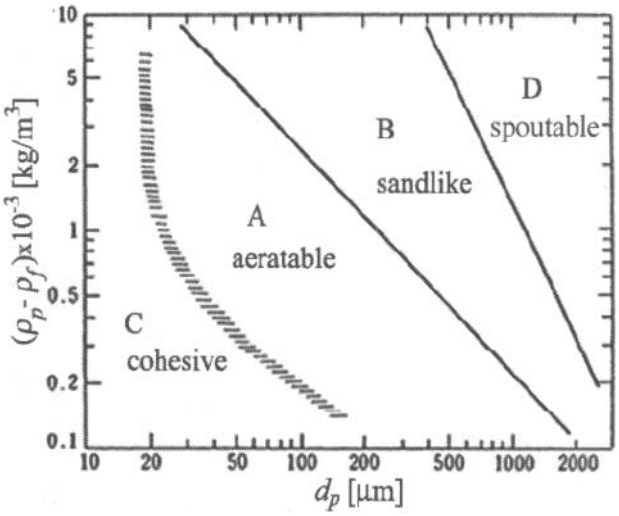

Fig. 1. - Powder classification diagram for fluidization by air – source: (Geldart, 1973).

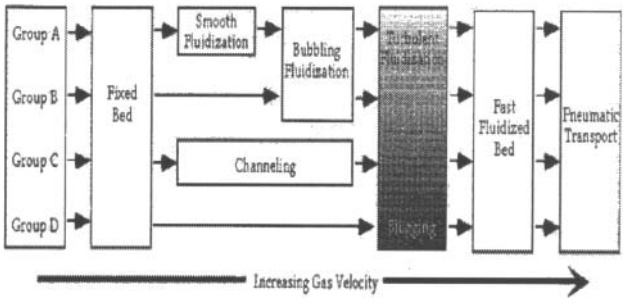

Fig.2. – Flow regime map for various powders.

Figure 2 summarized the fluidized bed hydrodynamics related with powders classified according to Geldart's criteria.
Once the velocities associated with each mode of operation are determined, the pressure drop of the regime is calculated and the gas-solid flow is predicted using the modeling and software adequated to optimize the industrial installation.

Minimum fluidization velocity calculation

This is generally defined as minimum superficial velocity at which the drag force and the upward buoyant force due to the fluid is balanced by the weight of the particles illustrated in figure 3.

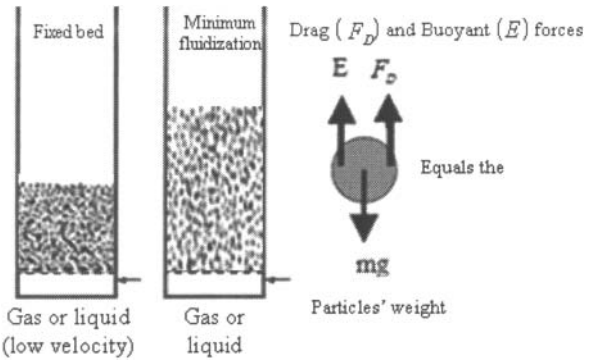

Fig. 3 – Fixed and a fluidized bed of particles at a minimum fluidization velocity – source: (Vasconcelos and Mesquita, 2011).

Theoretical model equations for predict: V_{mf}

Ergun (1952) developed, for fixed beds, a pressure-drop correlation at incipient fluidization based on drag force considerations of a single particle in a bed of particles of the same size and neglecting the buoyant force as follows in equation 1.

$$(1-\varepsilon_{mf})(\rho_s-\rho_g)g = 150\frac{(1-\varepsilon_{mf})^3}{\varepsilon_{mf}^3}\frac{\mu_g V_{mf}}{(\varphi_s d_p)^2} + 1.75\frac{(1-\varepsilon_{mf})}{\varepsilon_{mf}^3}\frac{\rho_g V_{mf}^2}{\varphi_s d_p} = AV_{mf} + BV_{mf}^2 \quad (1)$$

Calculating C by equation 2 one gets an equation of second power, which the positive solution is calculated by equation 3.

$$C = (1-\varepsilon_{mf})(\rho_s-\rho_g)g \quad (2)$$

$$V_{mf} = \frac{-A+\sqrt{A^2+4BC}}{2B} \quad (3)$$

Where A and B are the viscous and the inertial factor of the Ergun equation, C is the weight per unit volume of the bed of particles.
Fluidization is related with small velocities, the factor B is negligible and the Ergun equation can be simplified with an error less than 5% related to equation 3 by the equation 4.

$$V_{mf} = \frac{C}{A} \Rightarrow V_{mf} = \frac{(\rho_s-\rho_g)g\varepsilon^3{}_{mf}(\phi_s d_p)^2}{150(1-\varepsilon_{mf})\mu_g} \quad (4)$$

The prediction of V_{mf} by Ergun's equation for pressure drop requires the knowledge of sphericity of the particle ϕ_s and bed voidage ε_{mf} .Many researchers have been trying to surpass the difficult to determine the voidage and sphericity of the particle, combining equations 1 and 2, plus the Arquimedes, Reynolds Froude's numbers with their experimental results adjusting their equations to predict V_{mf} as can be seen in table 1.

Authors	Equation	
Leva	$V_{mf} = 9.23\text{x}10^{-3} d_p^{1.82}\left(\frac{\rho_s}{\mu_g}\right)^{0.88}\left(\frac{\rho_s}{\rho_g}\right)^{0.94}$	(5)
Abrahamsen & Geldart	$V_{mf} = 9\text{x}10^{-4} d_p^{1.8}\left[(\rho_s-\rho_g)g\right]^{0.934}\rho_g^{-0.066}\mu_g^{0.87}$	(6)
Coltters & Rivas	$V_{mf} = 3.7774\text{x}10^{-5}\left(\frac{d_p^2(\rho_s-\rho_g)g}{\mu_g}\left(\frac{\rho_s}{\rho_g}\right)^{1.23}\right)^{0.603559}$	(7)
Wen & Yu	$V_{mf} = \frac{\mu_g}{\rho_g d_p}\left(\sqrt{33.7^2+0.0408\,A_r}-33.7\right)$	(8)
Miller & Logwinuk	$V_{mf} = 1.25\text{x}10^{-3}\left(\frac{d_p^2(\rho_s-\rho_g)^{0.9}\rho_g^{1.1}g}{\mu_g}\right)$	(9)

Table 1 - Semi-empirical equations for predicting minimum fluidization velocity V_{mf}

For an incipient fluidization, when the weight of particles equals the drag force, it is a good attempt to consider the porosity at the minimum fluidization velocity ε_{mf} equals or close the porosity ε of the fixed bed. The porosity of the fixed bed is calculated by the equation 10.

$$\varepsilon = 1-\frac{\rho_{bmv}}{\rho_s} \quad (10)$$

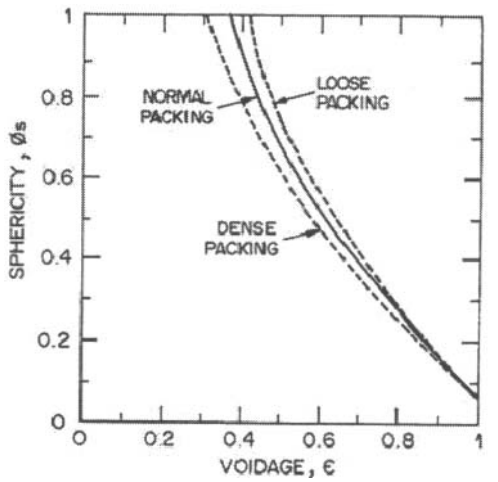

Fig. 4 - Voidage in uniformly sized and randomly packed beds- adapted from (Kunii and Levenspiel, 1991).

$$\rho_{bnv} = \frac{M_s}{V_{total}} \tag{11}$$

Where ρ_{bnv} is the non-vibrated bulk density, ρ_s is the solid real density derived in a laboratory by a pycnometer, M_s is the total mass of particles weighed on an electronic scale, V_{total} is the total volume of particles and voids in the sample previously weighed in on electronic scale, d_p is the particle mean diameter obtained by sieve analysis in a laboratory, ϕ_s is the particle sphericity, that can be estimated from figure 4 considering a normal packing bed of particles.

Based on the work of (Biswal *et al*, 2007) and data for alumina fluoride obtained upon a thesis by (Vasconcelos, 2011) for doctorate degree at Federal University of Pará, equation 12 was proposed to predict the minimum fluidization velocity.

$$V_{mf} = 0.21(A_r)^{0.25}\left(\frac{\phi_s}{1.05\varepsilon}\right)^{0.7}(d_p g)^{0.5} \tag{12}$$

Where:

Arquimedes Number: $$A_r = \frac{d_p^3(\rho_s - \rho_g)\rho_g g}{\mu_g} \tag{13}$$

And $\rho_g ; \mu_g ; g$ are respectively the real density and viscosity of the gas (air); acceleration due to gravity.

The experimental value of V_{mf} and minimum velocity of full fluidization V_{mff} are obtained using a permeameter as showed in figure 5 measuring the gas superficial velocity and the pressure drop through the bed of particles.

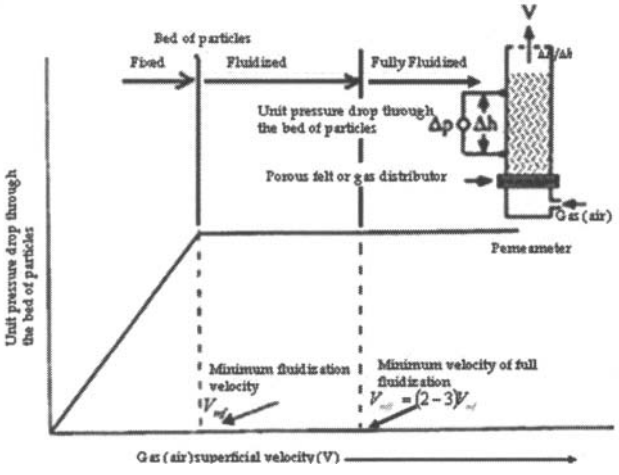

Fig. 5 – Pressure drop through a bed of uniformly particles versus superficial air velocity – source: (Mills, 1990).

Experimentals details

A schematic diagram of the experimental set-up is shown in figure 6. The arrangement of the permeameter made of fiberglass with acrylic sheets to allow visual observation of the fluidized particles. Two rectangular and one circular shape permeameters were built as illustrated in figure 7. Air flow rate is measured by rotameters with precision of ± 3% full scale and the pressure drop with the appropriate dust filter in the pressure taps is measured by digital pressure transmitters at a precision of ± 1% of full scale. Air at a temperature of 303 K, ($\rho_g = 1.189 kgm^{-3}$ and $\mu_g = 18.602x10^{-6} Pa.s$) under atmospheric pressure, used as the fluidizing medium was passed through a dust filter and humidity eliminator. The pressure was regulated at 2 bars in the inlet of the rotameters.

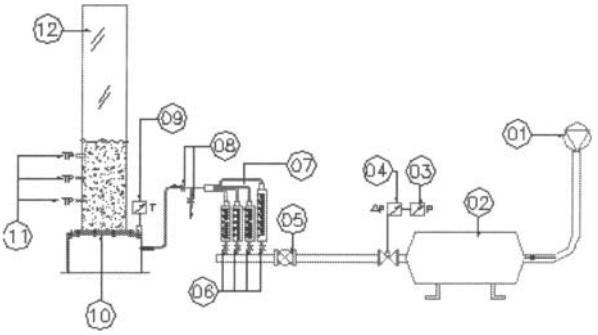

Fig. 6 – Experimental set-up: 1) air mover; 2) air receiver; 3) manometer; 4) air pressure regulator (0 – 3) bar; 5) ball valve; 6) air flow regulator; 7) rotameters (0 - 10; 0 - 25; 0 - 100; 0 - 700) LPM; 8) ball valves; 9) thermometer; 10) polyester porous membrane; 11) pressure drop transmitters (0 – 125; 0 – 1250; 0 – 5000) Pa; 12) permeameter.

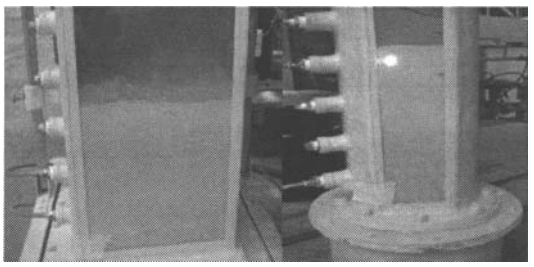

Fig. 7 – Permeameters used at Albras' laboratory to survey the minimum fluidization velocity of the powders used in the primary aluminum industry.

Diameter range (μm)	$\bar{d_p}i$ (μm)	Weight fraction x_i	$(x/\bar{d_p})i$
0 - 37	18.5	0.0465	0.002513
37 - 44	40.5	0.0395	0.000975
44 - 74	59.0	0.2743	0.004649
74 - 147	110.5	0.6027	0.005454
147 - 250	200.0	0.0365	0.000182
		$\sum(x/\bar{d_p})i$	0.001377
	$d_p(\mu m)$	$\bar{d_p} = 1/\sum(x/\bar{d_p})i$	72.6 ±2.7

Table 2 – Reacted alumina sieve analysis – 100 samples (minimum /maximum size and standard deviation): (68.68/78.23 and 2.7) μm) - source: (Vasconcelos, 2011).

Procedures

Reacted alumina is a mixture of multi-size particles, so before to start the fluidization survey, it was necessary to perform a sieve analysis to characterize the particles size as can be seen in table 2. Firstly, a determined initial mass (15 – 53 kg) of reacted alumina was introduced in the big rectangular 14" permeameter and (3 – 12 kg) in the circular 8" permeameter in order to ensure a bed height of about 0.1-0.4 m. Prior to actual fluidization tests, the bed was pre-conditioned to reduce the influence of interparticles forces in the dense bed packing. To this end, the superficial air velocity was rapidly increased around the predicted V_{mf} and then decreased in more or less 30 s. This procedure guarantees better homogeneity of the bed. After this preparation the air flow rate was increased in steps of 2 LPM (liters per minute) for about one minute and subsequently the pressure drop in bed of particles was measured until the pressure drop stays constant at a variation less than ± 5%. Then, the air stream was decreased in steps of 2 LPM until 0 LPM see figure 8. Each fluidization cycle test (batches of reacted alumina summarized in table 3) was repeated twice.

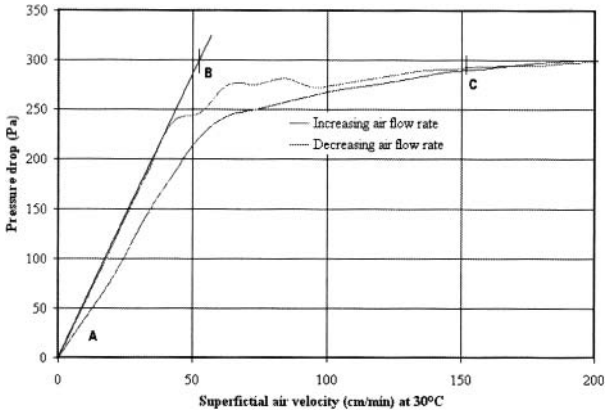

Fig. 8 – Experimental pressure drop in the bed of reacted alumina - (72.6 ± 2.7) μm /3387.3 $kg.m^{-3}$ versus superficial air velocity - source: (Vasconcelos, 2011).

From point A to point B in figure 8 the pressure drop increases with velocity (fixed bed). The transition from the stagnant bed to fluidized bed occurs at point B, i.e. at the minimum fluidization velocity V_{mf} (52.16 cm/min) intersection with the maximum pressure drop. From point B the pressure drop increases until point C, i.e. at the minimum velocity of full fluidization V_{mff} (153 cm/min). The pressure drop remains constant with variation around ± 5% of the maximum pressure drop. After point C the bed is fully fluidized.

The same procedures explained above were used to obtain the experimental values of V_{mf} and V_{mff} summarized in table 3 for others diameters of the alumina fluoride used at Albras aluminum smelter.

Results and Discussions

The minimum fluidization velocity was predicted using equation 12 proposed by (Vasconcelos, 2011) with an average absolute error less than 0.5% compare with the experimental showed in figure 8.

For the granulometries sub 37 μm (- 400 mesh), it was used a small rectangular permeameter illustrated in figure 9, because after more than 150 sieve analysis of the reacted alumina we got only one kilogram of this fraction to study. As can be observe in figure 9 it was impossible to determine the minimum fluidization velocity in this test due to channeling in the bed of particles.

The experimental data obtained for the minimum fluidization velocity V_{mf} were compare with the equations proposed by (Vasconcelos, 2011), (Ergun, 1952) and others researchers listed in table 1. The comparison of calculated and experimental V_{mf} for a stagnant bed of particles with the data related in table 2 is shown in table 4 with the respective absolute error (%) based on experimental value. Figures 10 and 11 show the graphic analysis.

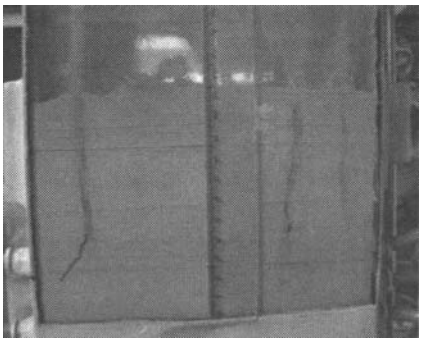

Fig. 9 – Permeameter of 50x200 mm used to reacted alumina sub 37 μm (Geldart group C).

Material Reacted alumina Mean diameter (μm)	Particle density kgm^{-3}	Bed Voidage (-)	Particle sphericity (-)	V_{mf} (cm/ min) Experimental
40.5	3310.3	0.709996	0.370	14
59.0	3336.1	0.715230	0.360	42
72.6	3387.3	0.716580	0.365	52
111.5	3381.9	0.707265	0.371	94
200.0	3263.0	0.598520	0.520	250

Table 3 – Parameters of the fluidized bed of alumina fluoride's particles - source: (Vasconcelos, 2011).

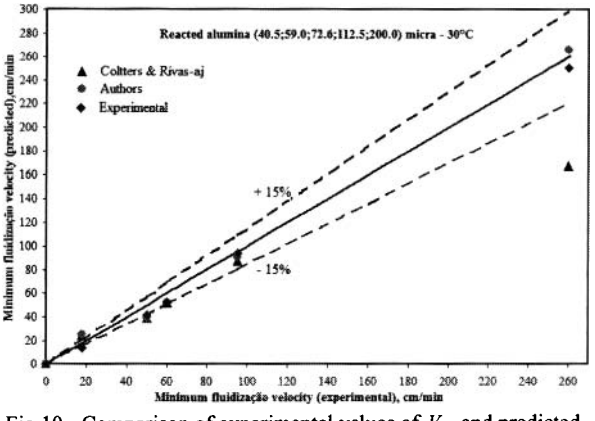

Fig.10 - Comparison of experimental values of V_{mf} and predicted by Vasconcelos and Coltters and Rivas.

Material Reacted alumina dp (μm)	V_{mf} (cm/min) (a)	(b)	(c)	(d)	(e)	(f)	(g)	(h)	Absolute error (%) based on exp. value (b)	(c)	(d)	(e)	(f)	(g)	(h)
40.5	14.00	25.36	18.74	16.93	14.12	24.90	10.40	11.13	81.14	33.86	20.92	0.86	77.86	27.86	19.78
59.0	42.00	39.70	39.44	33.84	28.00	39.60	22.23	23.79	5.48	6.10	19.43	33.33	5.71	47.10	43.36
72.6	52.00	52.16	63.19	50.18	41.36	52.00	34.26	36.61	0.31	21.52	3.50	20.46	0.00	34.11	29.60
111.5	94.00	90.85	147.53	109.16	89.20	87.00	80.39	86.02	3.35	51.62	16.12	5.10	7.45	14.48	8.49
200.0	250.00	266.09	380.39	305.60	246.95	167.80	247.97	267.99	6.43	52.15	22.24	1.22	32.88	0.81	7.20

(a) Experimental; (e) (Abrahamsen and Geldart, 1980);
(b) Thesis; (f) (Colters and Rivas, 2004) ajusted;
(c) (Ergun, 1952); (g) (Wen and Yu, 1996);
(d) (Leva, 1959); (h) (Miller and Logwinuk, 1951).

Table 4 – Comparison of experimental and predicted minimum fluidization velocity for stagnant bed of reacted alumina – source: (Vasconcelos, 2011).

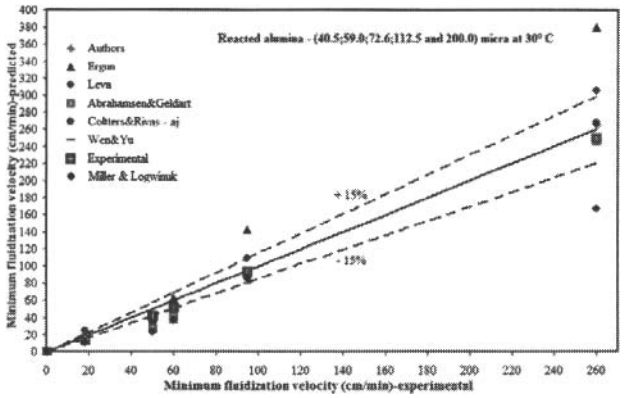

Fig. 11 – Comparison of experimental values of V_{mf} with predicted values.

Other important parameters are the non aerated and aerated angle of repose illustrated in figure 12 to estimate flowability of the powder to be transport in conventional or new development of air fluidized conveyors of multiples outlets.

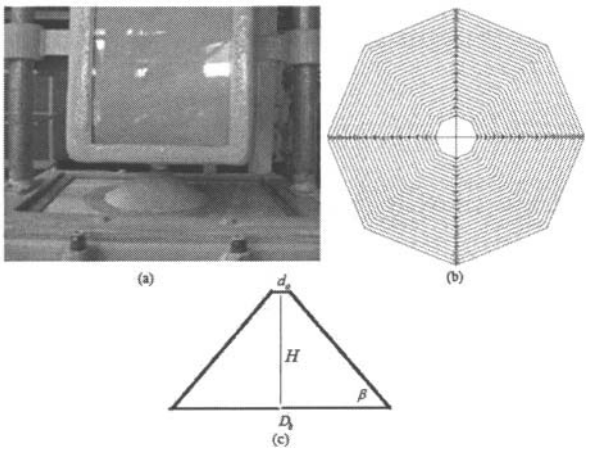

Fig. 12 – Apparatus to measure the non-aerated and aerated angle of repose – reacted alumina non-aerated angle (30.98 ± 0.42) °.

The measurement of the angle of repose β using the apparatus (a) of figure 12 and equation 14 follows the procedures:
Adjust the height (H), observe the diameter (D_b) which the powder rests in the circles of figure 12b. The diameter (d_o) of the orifice's discharge used in equation 14 is adjusted according the powder Geldart's classification.
10 measurements were made using reacted alumina in the apparatus showed in figure 12c and this angle was calculated by equation 14 obtaining $\beta = (30.98 \pm 0.42)°$ for reacted alumina.

$$\beta = ATAN\left(\frac{2H}{D_b - d_o}\right) \tag{14}$$

The base of figure 12c is a polyester porous felt with rulers of 300 mm in the axes x and y. The aerated angle of repose becomes zero at the minimum velocity of full fluidization V_{mff}, which is around $2.15\,V_{mf}$ for reacted alumina. The author proposes the equation 15 to predict the aerated angle of repose of the reacted alumina.

$$\beta_{fluidizado} = \beta\left(1 - 0.43\frac{V}{V_{mf}}\right)^2 \tag{15}$$

Figure 13 shows graphically the behavior of the aerated angle of repose for reacted alumina proposed by Vasconcelos (2011) and Kozin and Baskakov (1966) by the equation 16.

$$\beta_{fluidizado} = ATAN\left[\tan\beta\left(1 - \frac{V}{V_{mf}}\right)^2\right] \tag{16}$$

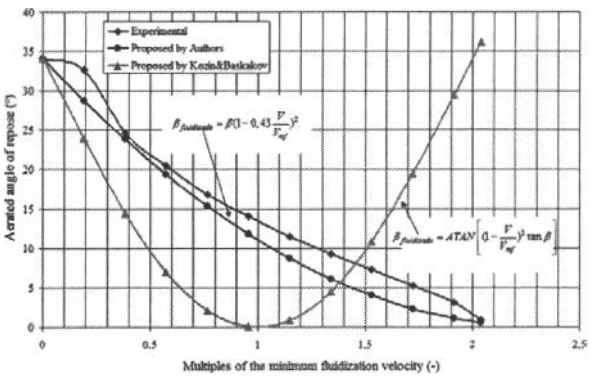

Fig. 13 – Aerated angle of repose versus multiples of superficial fluidization velocity – reacted alumina.

Figure 13 illustrates the round non-metallic special air slide developed upon a thesis of doctorate by Vasconcelos (2011). This air slide named Air Fluidized Conveyor can transports fluidized powders even in upward direction due to its geometry that favor the gravity force in all angle of inclination. This equipment has the possibility for multiples outlets and can be manufactured as smaller as 1" internal diameter.

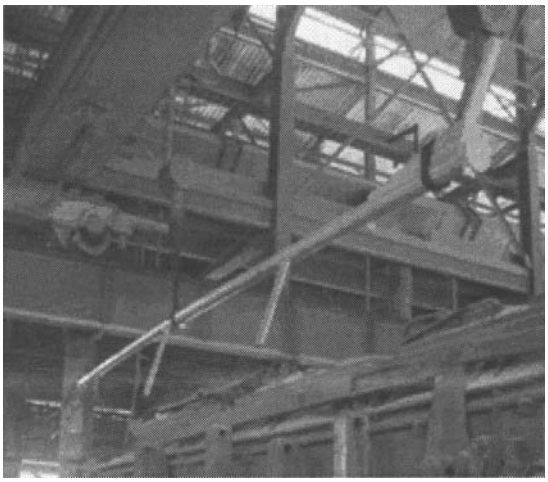

Fig. 13 – Albras' (Air Fluidized Conveyor) of three outlets.

Conclusions

Experiments were carried out with reacted alumina and four fractions of this alumina in the fluidization laboratory erected at Albras smelter to survey the alumina rheology in order to optimize energy consumption of the state of art Air Fluidized Conveyor developed showed in figure 13.

An equation was developed to predict the minimum fluidization velocity upon a thesis by (Vasconcelos, 2011) compared with other researchers and the experimental values. The predicted values by Vasconcelos and Coltters & Rivas adjusted by the experimental result for reacted alumina $d_p = 72.6\mu m$ are quite satisfactory with the experimental results showing an error less than 0.5% as can see in table 4 and in figures 10 and 11.

The correlations of Abrahamsen & Geldart fit very well with fine powders of group C and A. The equations of Wen & Yu and Miller & Logwinuk show better results for large particles of group B and D. The equation of Leva fit better with group B powders.

The correlations of Ergun and Vasconcelos are very sensitive to porosity and the sphericity of the particles and hence care should be taken to measure the porosity very accurately and also in estimate the sphericity using figure 4.

The proposed correlation by this paper could also find practical utility in designing and operations of fluidized bed for gas dry scrubbing to estimate the residence time of the particles in contact with gases and also optimized the size and energy consumption of air slides.

Acknowledgment

The authors would like to thanks Albras Alumínio Brasileiro SA for the authorization to public this paper, the Federal University of Pará for my doctorate in fluidization engineering and. My manager Marcelino Vasconcellos and the general managers Luís Carlos Carvalho Costa and Braz Mileo Ferraioli.

References

Abrahamsen , A. R. and Geldart, D. Behavior of gas fluidized beds of fine powders. I. Homogenous expansion, Powder technology, Vol. 26, 35, (1980);

Biswal *et al.*, Minimum fluidization velocities and maximum bed pressure drops for gas-solid tapered fluidized beds;

Coltters, R. and Rivas, A. L. Minimum fluidization velocity correlations in particulate systems, Powder Technology Vol. 147 pp. 34 – 48 (2004);

Ergun, S. Fluid Flow through Packed Columns, Chem. Engrg. Progress, Vol. 48, No. 2, pp. 89 – 94 (1952);

Geldart, D. Types of Gas Fluidization Powder Technology, 7, 285 – 292 (1973);

Kozin, V. E., Baskakov, A., Vuzov, P., Izv., Neft 1 Gas 91 (2) (1996).

Kunii, D. and Levenspiel O. Fluidization Engineering, second edition, Butterworth-Heinemann, Boston (1991);

Leva, M., Fluidization, McGraw-Hill, New York (1959);

Miller, C. O. and Logwinuk, A. K. Ind. Eng. Chem., 43 (1951) 1220;

Mills, D. Pneumatic Conveying Design Guide, Butterworths, London, (1990).

Vasconcelos, P. D. Doctorate Thesis, Federal University of Pará at Belém, 2011;

Vasconcelos, P. D. and Mesquita, L. A. Gas-solid flow applications for powder handling in industrial furnaces operations. Chapter 10 of the book Heat Analysis and Thermodynamics Effects, ISBN 978-953-307-585-3. Intech open access publisher, Rijeka, September (2011).